

The plots produced from the scans were then examined to obtain data on the pitting potential  $E_p$ , the range of perfect passivation, and the size of the hysteresis loop formed by the reverse scan.

Cyclic polarisation scans were carried out under various conditions:-

- Detailed tests under flow conditions at  $40^{\circ}\text{C}$  and  $1,75\text{ms}^{-1}$ .
- Limited tests under flow conditions at  $40^{\circ}\text{C}$  and  $1,0\text{ms}^{-1}$ ,  $2,5\text{ms}^{-1}$  and  $3.25\text{ms}^{-1}$ .
- Static, aerated at  $40^{\circ}\text{C}$ .
- Static, de-aerated at  $40^{\circ}\text{C}$ .
- Static aerated at  $5^{\circ}\text{C}$ ,  $22^{\circ}\text{C}$ ,  $30^{\circ}\text{C}$ ,  $50^{\circ}\text{C}$ , and  $60^{\circ}\text{C}$ .

These tests were to provide information on the pitting behaviour of the range of alloys under flow and static conditions as well as an indication of the effects of flow velocity and temperature.

#### 5.3.4 AERATION AND DE-AERATION

Full aeration of the water was assumed to prevail under flow loop conditions, since the outlet from the loop into the tank was above water level, and the returning water fell through air and created strong turbulence at the air/water interface in the tank.

Under static conditions aeration was achieved by bubbling compressed air through the water. Care was taken to ensure that no air bubbles impinged on either the corroding surface of the specimen or on the reference electrode.

The plots produced from the scans were then examined to obtain data on the pitting potential  $E_p$ , the range of perfect passivation, and the size of the hysteresis loop formed by the reverse scan.

Cyclic polarisation scans were carried out under various conditions:-

- Detailed tests under flow conditions at 40°C and  $1,75\text{ms}^{-1}$ .
- Limited tests under flow conditions at 40°C and  $1,0\text{ms}^{-1}$ ,  $2,5\text{ms}^{-1}$  and  $3,25\text{ms}^{-1}$ .
- Static, aerated at 40°C.
- Static, de-aerated at 40°C.
- Static aerated at 5°C, 22°C, 30°C, 50°C, and 60°C.

These tests were to provide information on the pitting behaviour of the range of alloys under flow and static conditions as well as an indication of the effects of flow velocity and temperature.

#### 5.3.4 AERATION AND DE-AERATION

Full aeration of the water was assumed to prevail under flow loop conditions, since the outlet from the loop into the tank was above water level, and the returning water fell through air and created strong turbulence at the air/water interface in the tank.

Under static conditions aeration was achieved by bubbling compressed air through the water. Care was taken to ensure that no air bubbles impinged on either the corroding surface of the specimen or on the reference electrode.

De-aerated tests were carried out only under static conditions. Argon was used to de-aerate the water and it was bubbled through the water for 1 hour before the specimen was immersed and then throughout the duration of the scan.

### 5.3.5 TEMPERATURE CONTROL

In the flow loop the water temperature was maintained at  $40 \pm 0,5^{\circ}\text{C}$  throughout the duration of the immersion and electrochemical tests.

In the static tests in the controlled temperature bath, the temperature was maintained within  $40 \pm 0,5^{\circ}\text{C}$  throughout these tests.

In the static electrochemical corrosion tests, various temperatures ranging from  $5^{\circ}\text{C}$  to  $78^{\circ}\text{C}$  were used. From ambient temperature upwards an immersion heater with a thermostat and a stirrer were used to give temperature control within  $\pm 0,5^{\circ}\text{C}$ . Below ambient temperature the same equipment was used with additions of ice to the bath water. This also gave temperature control within  $\pm 0,5^{\circ}\text{C}$ .

## 5.4 TOTAL IMMERSION TESTING

### 5.4.1 SPECIMEN PREPARATION

Two approaches were used for specimen preparation for immersion testing. The first involved grinding and polishing the specimens and the second

was to expose them with the surface finish with which the material came from the mill.

The first procedure was as follows:-

- Grind specimens with 120 grit SiC paper.
- Wet polish specimens with 600 grit SiC paper.
- Rinse in distilled water.
- Rinse in acetone.
- Dry in dessicator for 24 hours.
- Weigh specimens to 0,001g.

Alclad specimens were not ground with 120 grit paper; they were only very lightly abraded with 600 grit paper.

Both the "ground" finish and "mill finish" specimens had their edges rounded with a fine file to decrease sharp edge effects. These tend to be regions at which preferential corrosion takes place.

All specimens then had their edges coated with a masking compound to try to avoid edge effects. The edges of the hole in the static immersion coupons were also masked. As the Alclad specimens only had cladding on one face, the non-clad side was also masked. The points of contact between the flow immersion specimens and their holders in the flow loop were coated with the masking compound to prevent crevice effects.

#### 5.4.2 SPECIMEN EXPOSURE

The static immersion test coupons were suspended in the tanks using glass hooks. The flow loop immersion specimens were clamped inside the holders in Test Section 1.

In the first test programme (ERPM Hercules Shaft Water) the exposure time was 3 weeks, whilst in the second test programme (Freddies No. 5 Shaft water) the exposure time was 6 weeks.

#### 5.4.3 SPECIMEN CLEANING

After exposure the specimens were removed from the tanks and flow loop and photographed immediately. They were then cleaned before re-weighing and examination. The cleaning procedure from ASTM D2688 (49) was as follows:-

- The coupons were scraped with a plastic knife and scrubbed dry with a nylon brush. On these specimens the corrosion products were collected for analysis. Where two distinct corrosion products were observed, they were collected separately.
- The specimens were then immersed in a chromic acid / phosphoric acid<sup>(\*)</sup> solution at 25°C for 30 min.
- During immersion in the acid each specimen was scrubbed twice with a nylon brush.

---

(\*) - 30g CrO<sub>3</sub> + 500ml of distilled water, add 36ml of H<sub>3</sub>PO<sub>4</sub> (specific gravity 1,689), dilute with distilled water to make 1l.

- They were then rinsed in tap water, followed by a rinse in distilled water and then a final rinse in acetone.

- The specimens were then dried between paper towels and stored in a desiccator for 1 hour.

- All the coupons were then re-weighed to find the mass loss.

To determine the mass loss as a result of the cleaning procedure, uncorroded specimens were first degreased in acetone, weighed and then subjected to the same cleaning procedure as the corroded specimens. The mass loss found due to the cleaning procedure was then used to correct the mass loss found with the corroded specimens.

#### 5.4.4 SPECIMEN EXAMINATION

After cleaning and weighing, the specimens were photographed, and then then visually examined to reveal all features of the corrosion which had taken place. Pit depths were measured using a dial gauge with a probe tip. First the deepest pit was found and then pit depth measurements were made every 10mm along the length of the specimens, on both faces. As the flow loop specimens had been mounted with one face up and the other down, a comparison of average and maximum pit depths for pits growing in each direction could be made.

Samples of each of the aluminium alloys were mounted in a cold set resin, wet polished to 1200 grit, then polished with  $3\mu\text{m}$   $\text{CaCO}_3$  and then polished with  $0,2\mu\text{m}$  diamond paste on a lapping wheel, then etched with Keller's reagent to show the microstructure. Sections were then cut through a selection of pits in the different alloys and mounted and polished as described above. These specimens were then carbon coated for examination using a light microscope and the SEM.

#### 5.4.5 CORROSION PRODUCT ANALYSIS

Samples of corrosion product were first analysed using a X-ray diffractometer. As no useful results were obtained, EDAX analysis was then performed. To prepare the samples, the powders were cemented to carbon mounts using a carbon paste. They were then coated with carbon to prevent charging with static electricity in the SEM. The spectrum for each element was obtained and the spectra were then processed to gain semi-quantitative results. Calibration was obtained by the use of a Co standard.

#### 5.4.6 TENSILE TESTING

To determine the loss of strength due to pitting and general corrosion, tensile tests were performed on the corroded specimens. Uncorroded specimens were also tested to provide a basis for comparison. The tensile test specimens were machined from the immersion coupons.

The tensile specimens were strained at a strain rate of  $5,5 \text{ mm min}^{-1}$  and plots of load against time were obtained. The cross sectional dimensions of the specimens were measured to 0,01mm and the ultimate tensile stress and percentage elongation at fracture were calculated. The percentage change in tensile strength due to corrosion was then evaluated.

## 5.5 MICROBIAL CONTROL

To decrease the possibility of microbial effects, the water in the flow loop and in the immersion tanks were dosed with a biocide - Chemserve Bioshock™.

For testing carried out in Hercules Shaft Water an initial dose of 300mg/ℓ was used followed by a weekly dose of 20mg/ℓ.

In the second test programme an initial dose of 400mg/ℓ was used, followed by weekly doses of 50mg/ℓ.

## 5.6 WATER COLLECTION

For both mine waters used, the collection procedure was the same. A 1000ℓ galvanised mild steel tanker trailer was taken to the mine. It was rinsed out with mine water and then filled. On return to the laboratory, the water was left to stand for 1 week for any solids to settle out before being transferred to the experimental apparatus. The mines had already treated the waters with flocculant to settle out solids and with lime to achieve a near neutral pH.

## 6.0 RESULTS AND DISCUSSION

### 6.1 TESTS CONDUCTED IN ERPM, HERCULES SHAFT WATER

This mine water is typical of the East Rand being high in sulphates with medium chloride levels. Pitting can be expected even with these levels of chlorides. The pH levels of the water in this mine are regularly adjusted to near neutral with lime. Flocculants are added to remove suspended solids. An analysis for the water is given in the table below:-

Table 6.1 Analysis of Hercules Shaft Water.

Component	Concentration*
pH	5,95
Total Hardness	1588
Ca Hardness	1123
'M' Alkalinity	40
Chloride	111
Calcium	448
Magnesium	113
Sodium	148
Sulphate	1775
Nickel	4,0
Copper	0,25
Conductivity	110mS/m

\* - in ppm where applicable

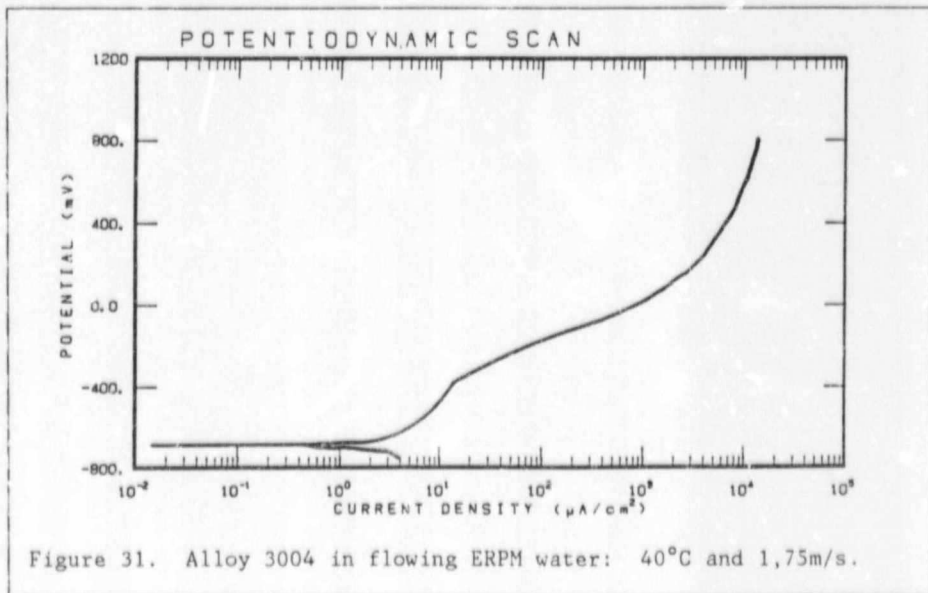
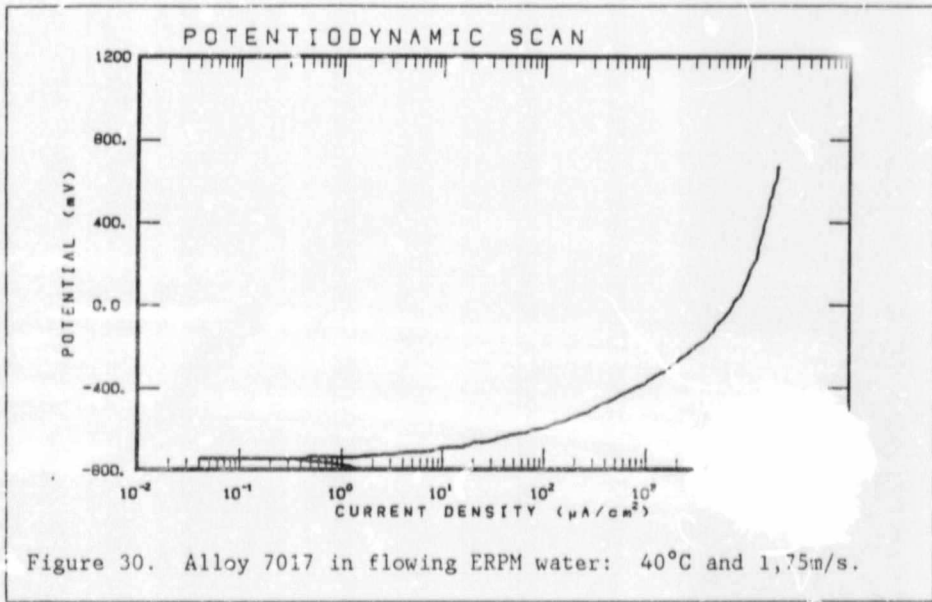
The pH is somewhat acid at 5,95, but this is still well within the pH 4,5 to 8,5 range for aluminium to exhibit passive behaviour, pitting corrosion can therefore be expected to be the dominant mode (if any) of corrosion.

### 6.1.1 POTENTIODYNAMIC SCANS - FLOW CONDITIONS, HERCULES WATER

All the aluminium alloys with the exception of 7017 (Figure 30) exhibited a region of spontaneous passivation before pitting occurred. This region was fairly limited and the corrosion currents were usually around  $10\mu\text{A}/\text{cm}^2$  when pitting occurred, a typical example is shown in Figure 31. Summarised data from the tests are given in Table 6.2.

Table 6.2 Potentiodynamic scan results - flowing Hercules Shaft water at 40.°C.

Alloy	Average Corrosion Potential (mV)	Average Corrosion Rate ( $\mu\text{m}/\text{yr}$ )
1200	-670	40,6
3004	-704	29,2
6063TB	-692	48,3
6063TF	-602	19,3
7017	-757	99,1
3CR12	-60	11,9
316L	-43	0



Alloy 7017 showed a very high corrosion rate and this could be seen on the specimen with the large amount of material removed. The remaining alloys corroded at rates in the 20 to 50 $\mu\text{m}/\text{yr}$  range, all being low enough for most service applications in this water. 3CR12 had a very low corrosion rate at approximately 12 $\mu\text{m}/\text{yr}$  and the general corrosion rate of type 316L stainless steel was too low to be measured - effectively zero. These corrosion rates only apply to general corrosion and give no information on the pitting behaviour of these materials. Both 3CR12 and 316L exhibited typical active-passive behaviour, with large passive ranges (described later in section 6.1.2).

#### 6.1.2 CYCLIC POLARISATION SCANS - FLOWING HERCULES WATER

Although all the aluminium alloys other than 7017 showed passive potential ranges, there are no reverse portions of the curves intersecting with the forward portions of the curve. This indicates that no potential ranges existed where pitting would neither initiate nor would existing pits cease to grow i.e. distinct pitting tendencies exist.

The pitting potential ( $E_p$ ) and the protection potential ( $E_{pp}$ ) are both somewhat dependant on the scan rate and  $E_{pp}$  is partially dependent on the current density at which the scan is reversed. A very high current density would cause the formation of numerous well established pits and hence the alloy may not be able to re-passivate. However, by using the same procedure for all the alloys, comparisons between the different materials may be made. The following table summarises the results of these tests.

Table 6.3 Results of cyclic polarisation scans in flowing Hercules water at  $1,75\text{ms}^{-1}$  and  $40^\circ\text{C}$ .

Alloy	Corrosion Potential (mV)	Passive Range (mV)	Perfectly Passive Range (mV)	Hysteresis Loop
1200	-670	412	0	Infinite
3004	-704	363	0	"
6063TE	-692	739	0	"
6063TF	-602	264	0	"
7017	-757	0	0	"
3CR12	-60	1206	1008	Medium
316L	-48	1316	1316	None

These results show that although a passive range exists where pits are not likely to initiate, if some pits do initiate, they will continue to grow and not repassivate. Alternatively, these results indicate that there are no anodic potentials at which pits will **not** initiate or propagate.

### 6.1.3 POTENTIODYNAMIC SCANS - STATIC HERCULES WATER

These tests were all carried out under fully aerated conditions and the results are summarised in the following table.

Table 6.4 Results of Potentiodynamic scans in static Hercules water at 40°C.

Alloy	Average Corrosion Potential (mV)	Average Corrosion Rate ( $\mu\text{m}/\text{yr}$ )
1200	-647	16,1
3004	-632	29,3
6063TB	-630	17,7
6063TF	-625	7,4
7017	-735	274,2
3CR12	-38	6,9
316L	-36	5,3

Overall the corrosion rates were lower than those obtained under flow conditions and as before alloy 7017 has a considerably higher corrosion rate than any other alloy. With the exception of alloy 7017, the **general corrosion** rates of the aluminium alloys are small enough to be insignificant in most general mining applications. These rates however bear no relationship to pitting rates.

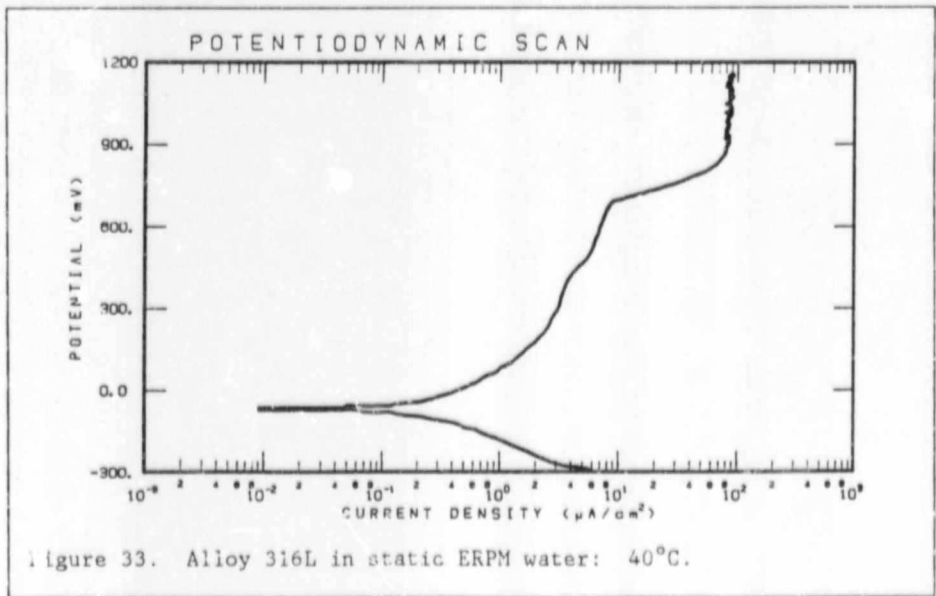
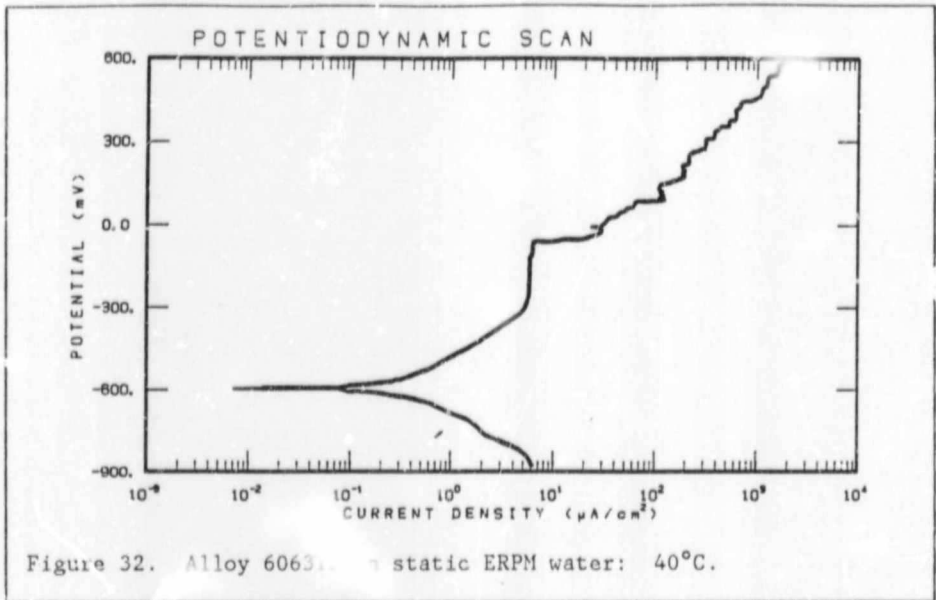
The passive ranges were generally very well defined as can be seen in Figure 32. Figure 33 shows the potentiodynamic curve produced with 316L stainless steel with a large passive region which contrasts with Figure 34 (alloy 7017) where there is no passive region at all.

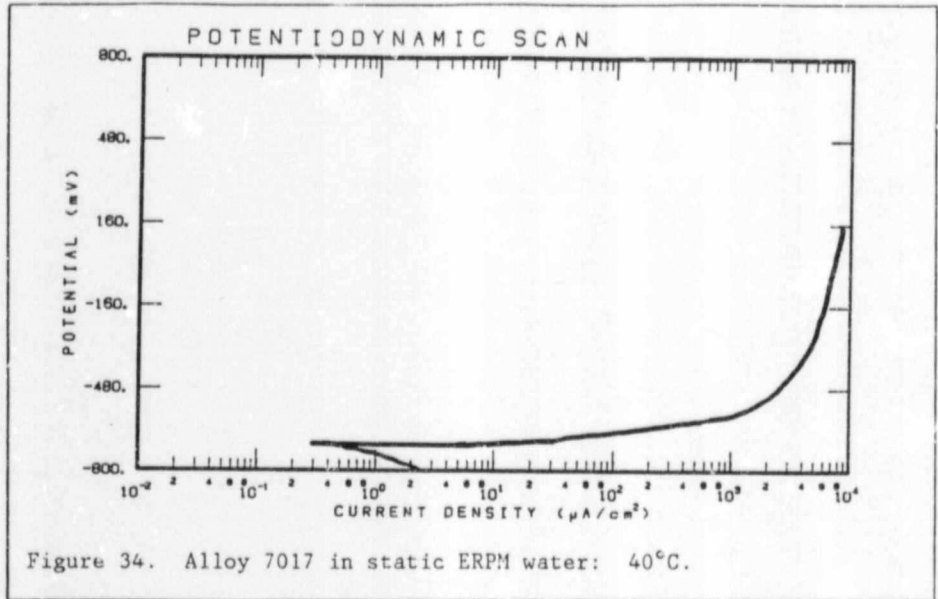
Table 6.4 Results of Potentiodynamic scans in static Hercules water at 40°C.

Alloy	Average Corrosion Potential (mV)	Average Corrosion Rate ( $\mu\text{m}/\text{yr}$ )
1200	-647	16,1
3004	-632	29,3
6063TB	-630	17,7
6063TF	-625	7,4
7017	-735	274,2
3CR12	-38	6,9
316L	-36	5,3

Overall the corrosion rates were lower than those obtained under flow conditions and as before alloy 7017 has a considerably higher corrosion rate than any other alloy. With the exception of alloy 7017, the **general corrosion** rates of the aluminium alloys are small enough to be insignificant in most general mining applications. These rates however bear no relationship to pitting rates.

The passive ranges were generally very well defined as can be seen in Figure 32. Figure 33 shows the potentiodynamic curve produced with 316L stainless steel with a large passive region which contrasts with Figure 24 (alloy 7017) where there is no passive region at all.





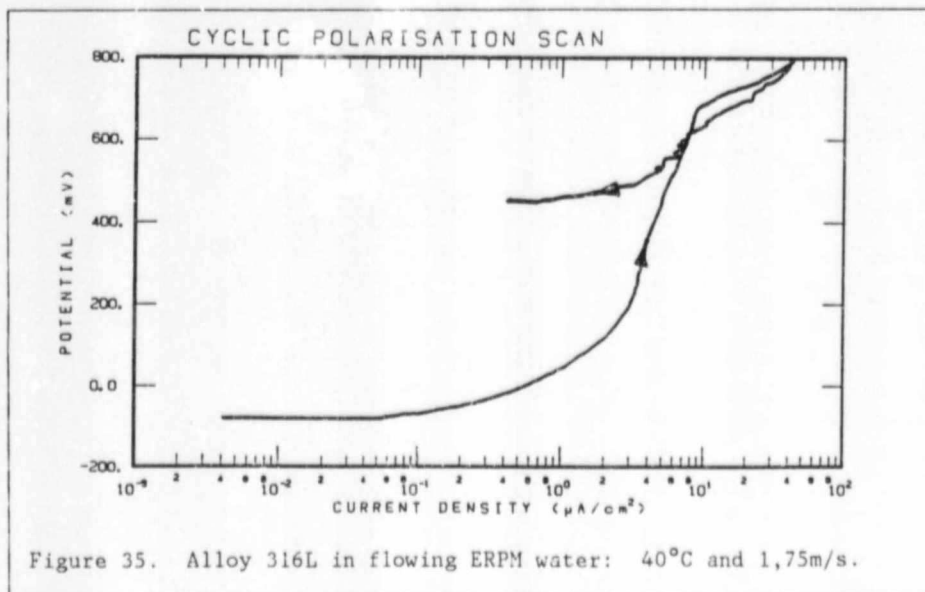
#### 6.1.4 CYCLIC POLARISATION SCANS - STATIC HERCULES WATER

The passive ranges observed were similar to or smaller than those found under flow conditions. The average results are given in Table 6.5.

The same comments about the dependence of these results on the scan rate and the current density at the reversal point, made in section 6.1.2 apply here. The trends are similar, with alloy 6063TB having the largest passive range (480mV) of the aluminium alloys. The two ferrous alloys had large perfectly passive ranges with small hysteresis loops. Figure 35 shows the cyclic polarisation curve for type 316L stainless steel under these conditions. The passive and perfectly passive ranges for these ferrous alloys are smaller under static conditions than with flowing water. This is an example of flow being beneficial in the prevention of the build up of local concentration cells for the initiation of pitting.

Table 6.5 Results of cyclic polarisation scans in static Hercules water at 40°C.

Alloy	Corrosion Potential (mV)	Pitting Potential (mV)	Passive Range (mV)	Perfectly Passive Range (mV)	Hysteresis Loop
1200	-647	-397	250	0	Infinite
3004	-632	-413	219	48	"
6063TB	-630	-150	480	0	"
6063TF	-547	-157	390	0	"
701,	-735	-	0	0	"
3CR12	-38	645	683	583	small
316L	-36	694	730	647	small



Alloy 3004 does have a region of perfect passivity, albeit very small (48mV). However, the large hysteresis loop indicates poor crevice cor-

rosion resistance and very little tendency for pits to passivate once formed. This is true for all the aluminium alloys which show a distinct tendency to undergo crevice attack under these test conditions.

#### 6.1.5 TOTAL IMMERSION TESTS - FLOW CONDITIONS.

Immediately after the specimens were removed from the flow loop they were visually examined and photographed.

They were all seen to have numerous small areas of a white corrosion product on a background of grey or black. The upper surfaces of the specimens are shown in Figure 36. The first three specimens from the left were in mill finish form, and the remainder were those polished to 500 grit.

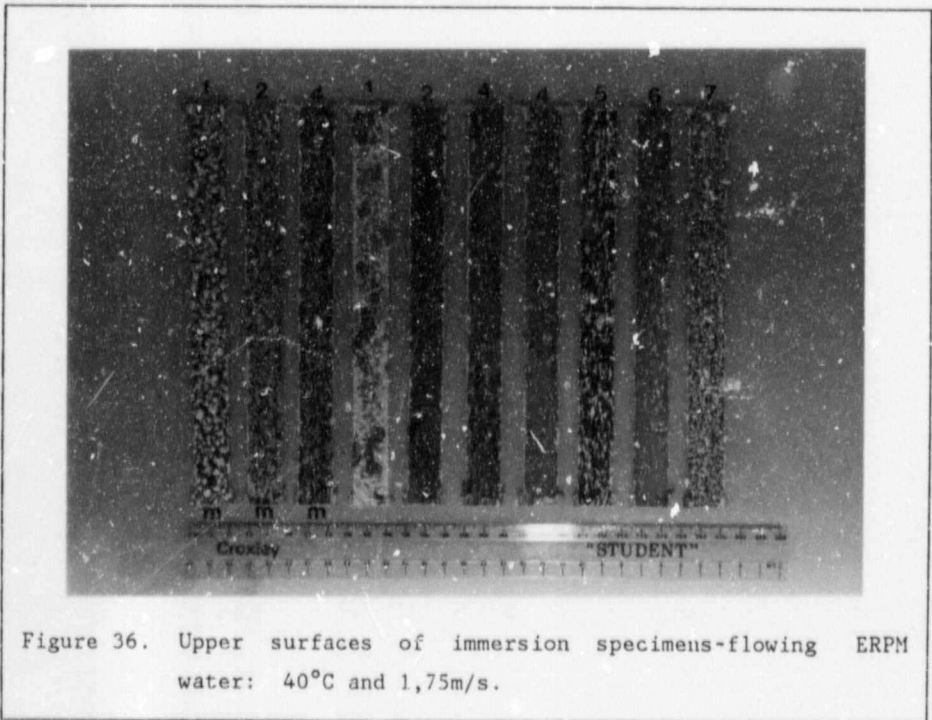


Figure 36. Upper surfaces of immersion specimens-flowing ERPM water: 40°C and 1,75m/s.

The mill finish specimens (Figure 37) appear to have experienced "worse" corrosion than the corresponding ground finish specimens (Figure 38), with the exception of the Alclad specimens.

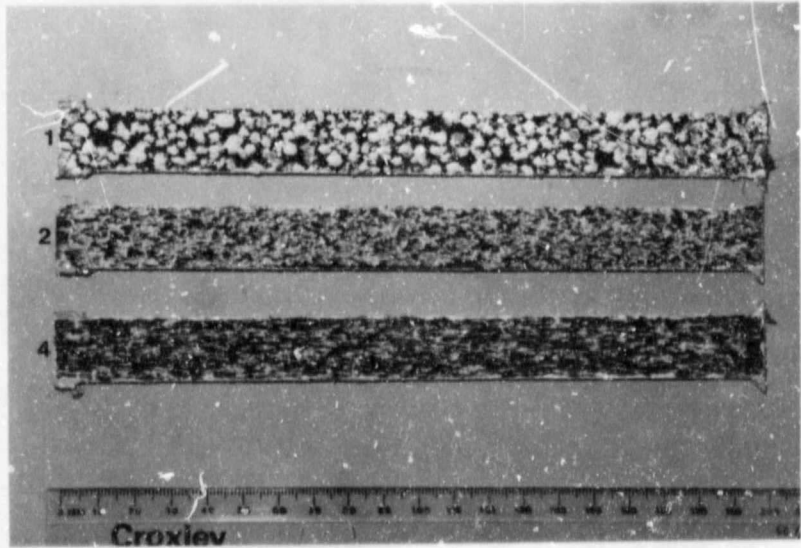


Figure 37. Immersion specimens-"Mill Finish"-Flowing ERPM water: 40°C and 1,75m/s.

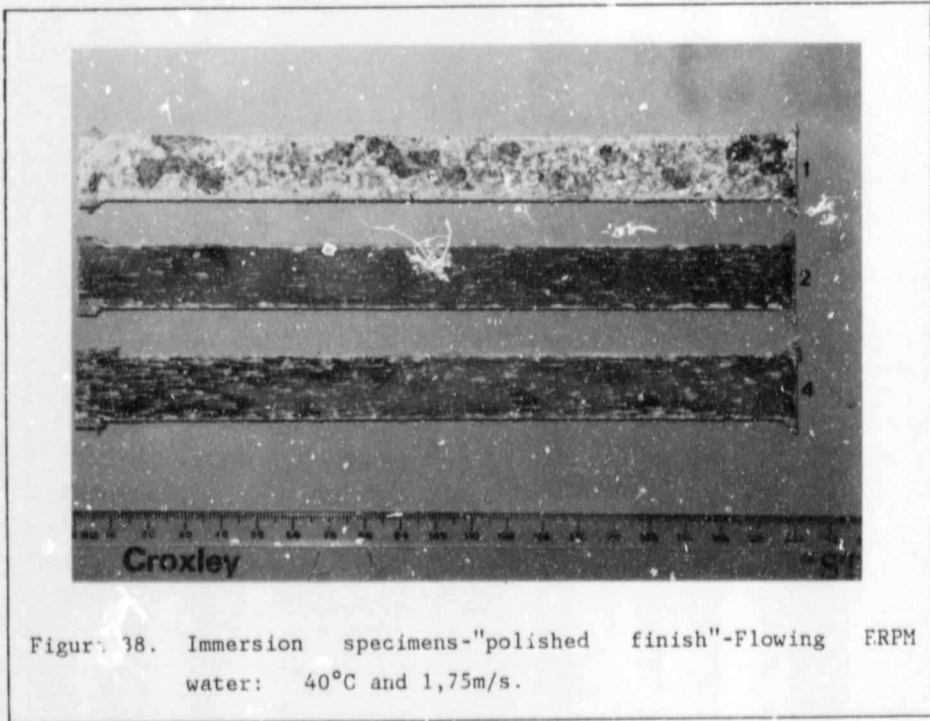


Figure 38. Immersion specimens-"polished finish"-Flowing FRPM water: 40°C and 1,75m/s.

The severe attack of the ground finish Alclad specimen was due to the non-clad reverse face **not** being coated with the masking lacquer. This caused galvanic corrosion of the cladding layer, which is anodic to the base metal. The protection given to the base metal can be seen in Figure 39 which shows the reverse face of the Alclad specimen. It is coated with a grey/black corrosion product but did not appear to have suffered pitting. This was confirmed once this surface coating was removed and the original polishing marks were still visible.

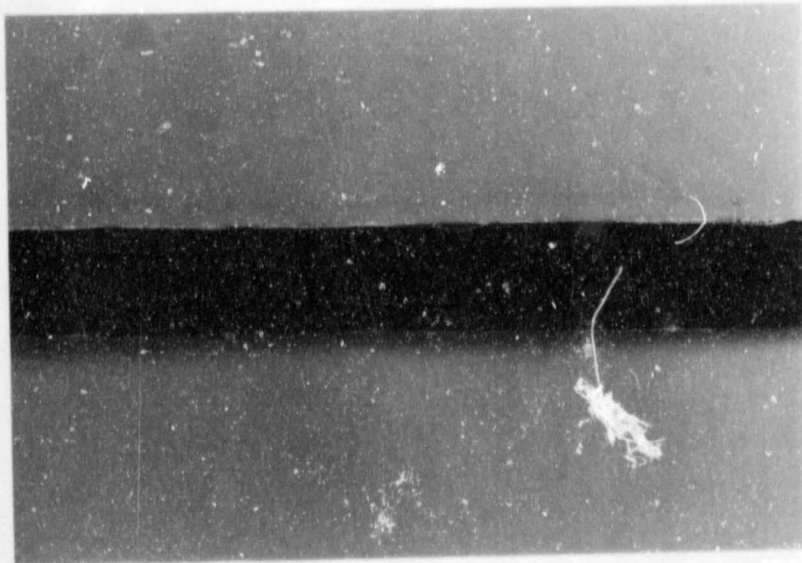
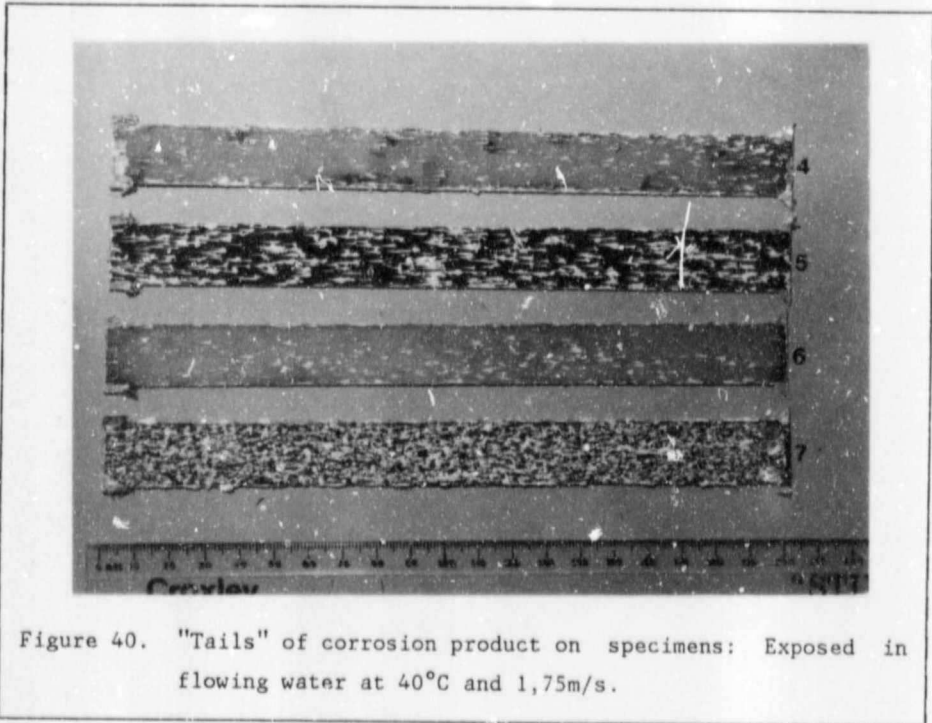


Figure 39. Non clad surface of Alclad specimen exposed in flowing ERPM water: 40°C and 1,75m/s.

That visual observation suggested higher corrosion rates of the mill finish specimens was borne out by the mass loss results, which will be discussed later. However there was no real difference in the average or maximum pit depths between the two finishes.

Figure 40 shows the upper face of alloys (top to bottom) 5251, 6063TB, 6063TF, and 7017. Note the "tails" of corrosion product from each pit indicating the direction of flow from right to left. Alloy 7017 appears to have experienced the most serious corrosion with more voluminous corrosion products found on its surface than with the other alloys.

Visual examination revealed no difference in the severity of corrosion between the upper and lower surfaces.



After cleaning in the chromic/phosphoric acids mixture the specimens were found to generally retain their polished surface. Figure 41 shows the upper surfaces of the specimens. The locations of the pits were as indicated by the corrosion product seen on the surfaces before cleaning. The "mill finish" Alclad specimen showed large scale removal of the cladding although shining portions of it remained. Due to the galvanic effects previously described, there was none of the original cladding surface left on the other Alclad specimen. Alloy 7017 had none of the original surface visible but no pits were visible. The surface was extremely rough and the corrosion appeared to be in the form of general corrosion with exfoliation.

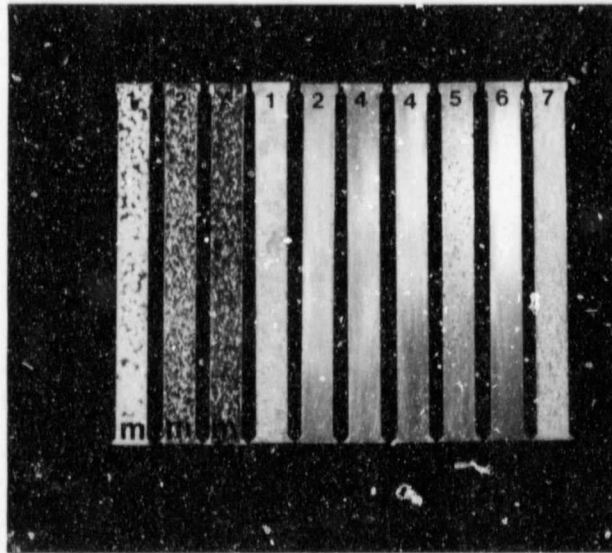


Figure 41. Immersion specimens from flowing ERPM water: After removal of corrosion product.

#### 6.1.5.1 Pit depth results

Although there were a larger number of pits present on the surfaces of the "mill finish" specimens than on their corresponding polished finish ones, the pit depths were similar as shown in Table 6.6.

Table 6.6 Pit depths from immersion specimens in flowing Hercules Shaft Water at 40°C.

Specimen	Pit Depth		
	Average (mm)	Maximum (mm)	Std. Deviation
Alclad mill	0,14	0,19	0,03
1200 mill	0,26	0,58	0,12
5251 mill	0,17	0,34	0,06
Alclad	(a)		
1200	0,26	0,52	0,07
5251	0,13	0,31	0,09
6063TB	0,35	0,62	0,11
6063TF	0,28	0,62	0,06
7017	(b)		

#### 6.1.5.2 Corrosion rate results - flowing water

These were calculated from the mass loss results obtained from the immersion specimens. There was a good correlation between the corrosion rates and the visual examination of the specimens. The following table gives the corrosion rates obtained.

---

(a) - all Alclad layer removed, (b) - general corrosion onl

Table 6.7 Corrosion rates from total immersion tests in flowing Hercules Shaft water at 40°C.

Alloy	Corrosion Rate ( $\mu\text{m}/\text{year}$ )
Alclad mill	2199,6
1200 mill	535,4
5251 mill	633,27
Alclad	3 321,0*
1200	346,5
5251	483,6
6063TB	1 003,7
6063TF	305,7
7017	2 199,6

Although drawn from only from one set of results, it appears that the "mill finish" specimen showed higher corrosion rates in this case. In the second series of tests (using Freddie's No.5 Shaft Water), a check was made to ascertain the effects (if any), of the position of the specimens in the test section, on corrosion rates. With these specimens, a maximum difference of 3% was found in the corrosion rates calculated for duplicate specimens in the positions where the "mill finish" specimens were positioned. These percentage differences were comparable with those found under static conditions; hence the difference in corrosion rates between "mill finish" and polished finish specimens was concluded to be due to their surface conditioning and not to their positions in the flow loop. The "mill finish" specimens had numerous scratches on their surfaces that were deeper than those left by the 600 grit paper on the polished specimens. These scratches and other mechanical damage to the surface would

---

\* This is an unrealistic value as it is partially due to galvanic corrosion.

provide likely points for pit initiation. Any foreign matter that was rolled into the surface during production would also provide preferential sites for corrosion.

#### 6.1.6 TOTAL IMMERSION TESTS - STATIC CONDITIONS

On removal, the specimens were found to be covered with a thin brown corrosion product and had localised areas of a very loosely adherent, voluminous, white corrosion product. Typical specimens are those shown in Figures 42 and 43. These photographs show the front and back surfaces respectively of pairs of specimens that were immersed in the same tank. As the specimens dried the brown appearance changed to a mainly grey colour. The right hand specimen of each pair is the "mill finish" specimen

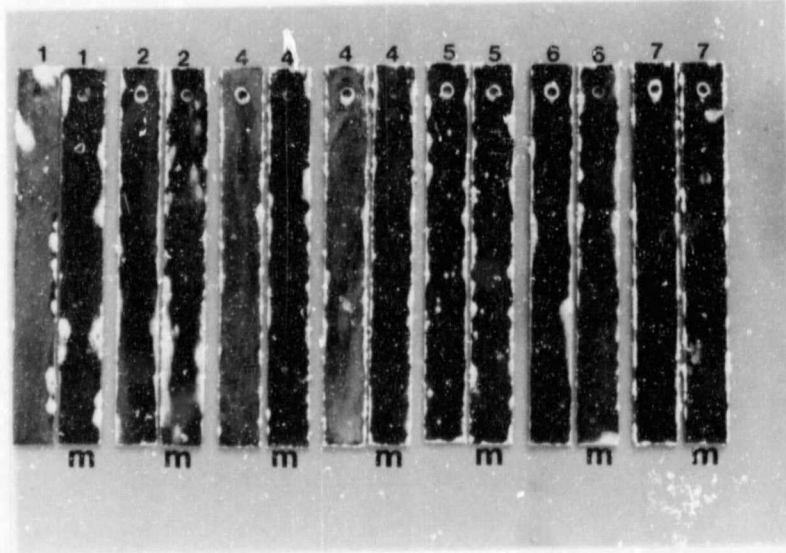


Figure 42. Front surfaces of specimens immersed in static ERPM water: 40°C. (m="mill finish").

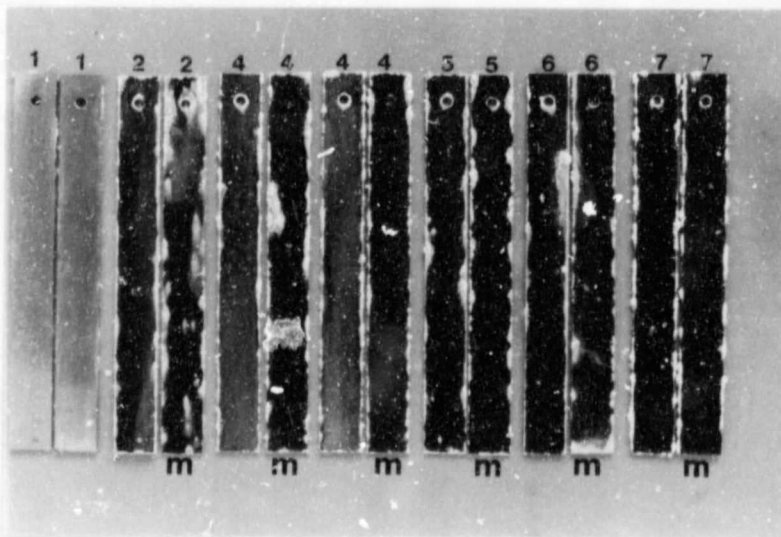
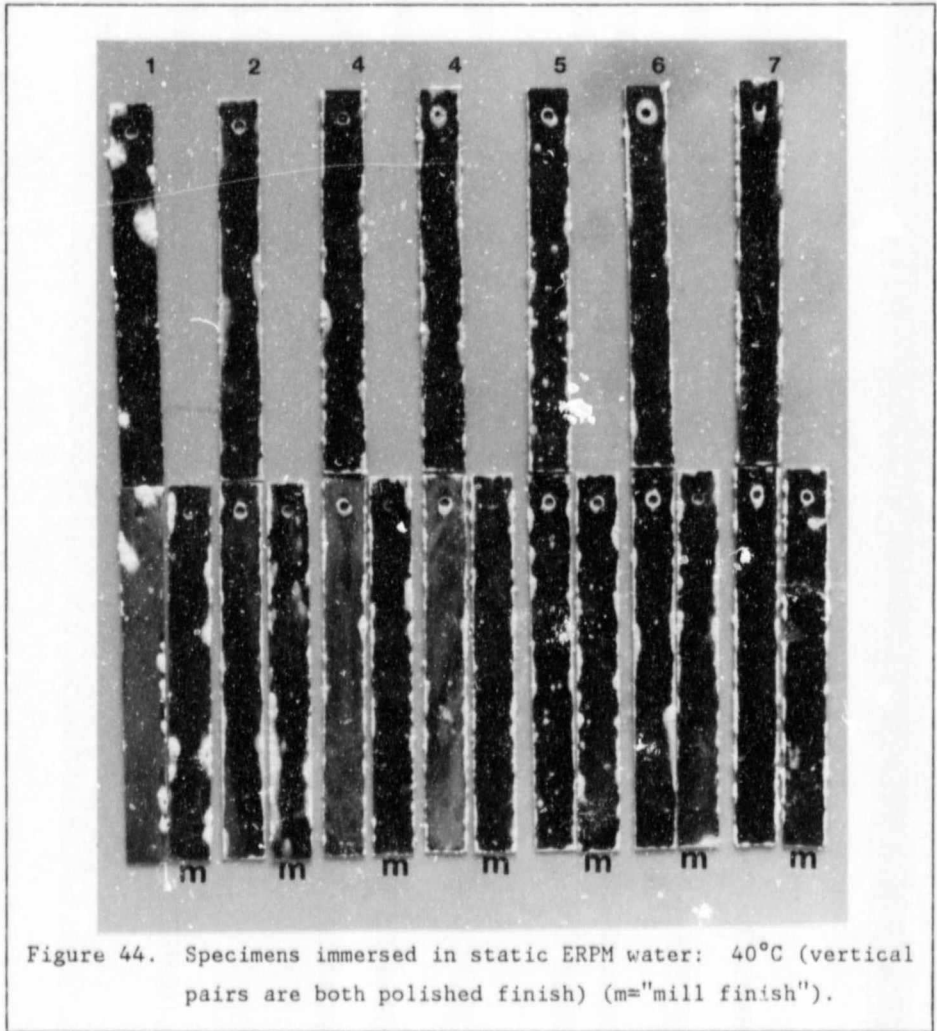


Figure 43. Rear surfaces of specimens immersed in static ERPM water: 40°C (m="mill finish").

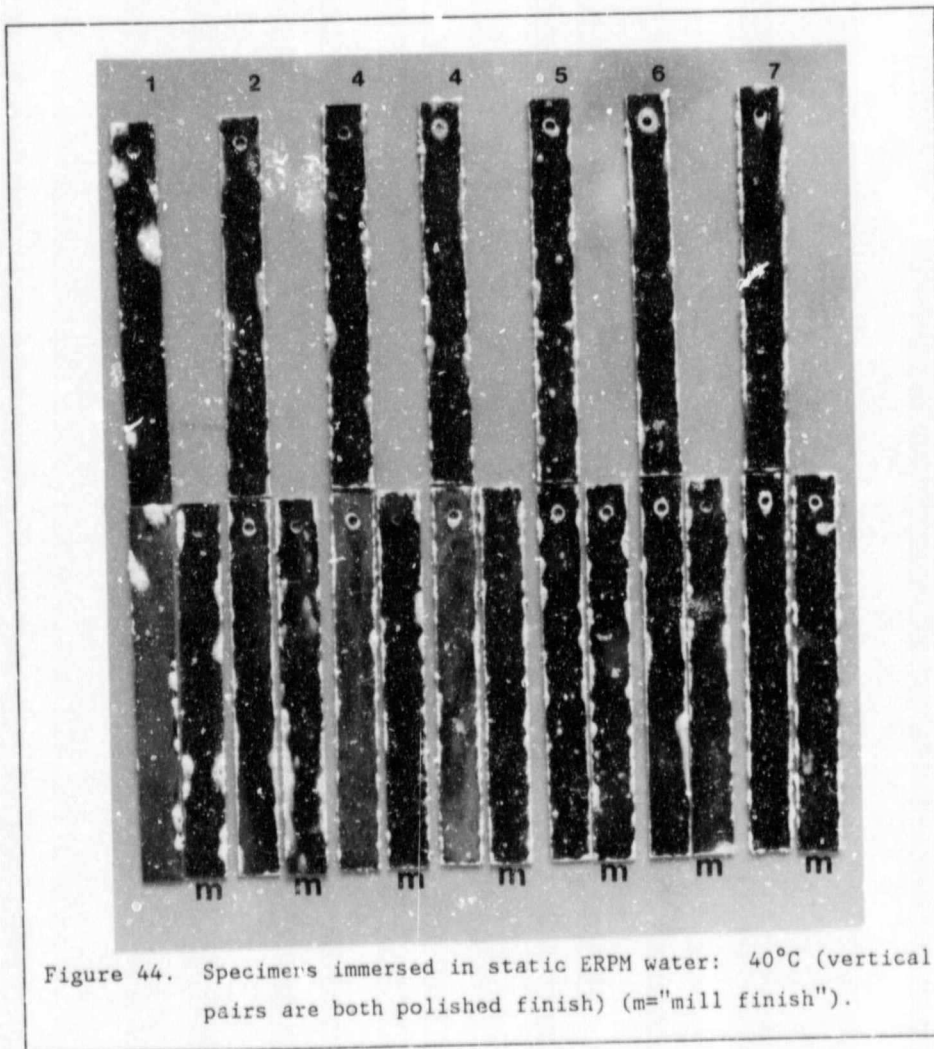
The corrosion product on the "mill finish" specimens surfaces appears to be rougher. However it is interesting to note that these specimens had a lower corrosion rate than the polished ones.

Figure 44 shows these specimens together with another set of polished finish specimens. Considerable corrosion has occurred at the specimen edges even though they were coated with a masking compound. This is due to partial lifting of the coating in places and the formation of localised crevices. However, examination of the severity of this corrosion at the edges does indicate that it was less severe than if the edges had not been masked.



This crevice attack confirms the electrochemical test results, which showed that these alloys had poor resistance to crevice corrosion in this environment.

After cleaning, the extent of the pitting was visible. It was far less than that seen on the specimens exposed under flow conditions. Figures 45 and 46 show surfaces of "mill finish" and polished finish specimens respectively. The original surfaces with scratches or polishing marks are clearly visible, except on alloy 7017. The "mill finish" alloy 7017



This crevice attack confirms the electrochemical test results, which showed that these alloys had poor resistance to crevice corrosion in this environment.

After cleaning, the extent of the pitting was visible. It was far less than that seen on the specimens exposed under flow conditions. Figures 45 and 46 show surfaces of "mill finish" and polished finish specimens respectively. The original surfaces with scratches or polishing marks are clearly visible, except on alloy 7017. The "mill finish" alloy 7017

specimen had been machined on one surface and the corrosion had clearly followed the line of the machining marks as expected.

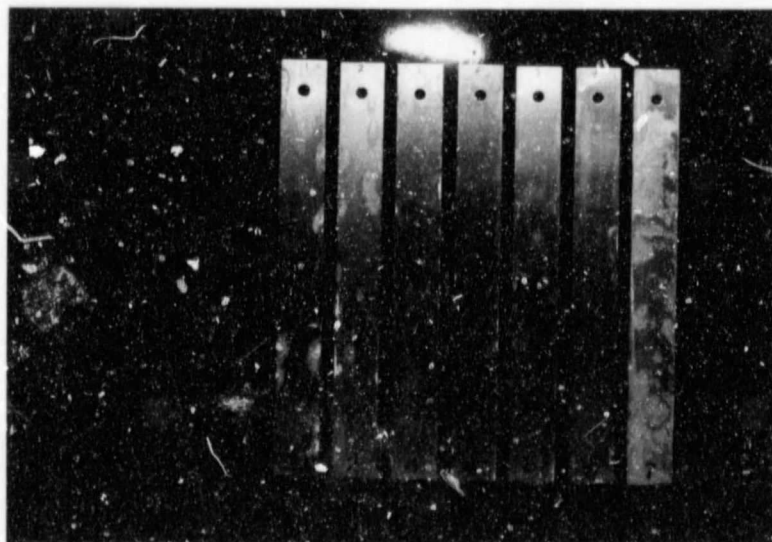


Figure 45. "Mill Finish" specimens exposed in static ERPM water: 40°C, after cleaning.

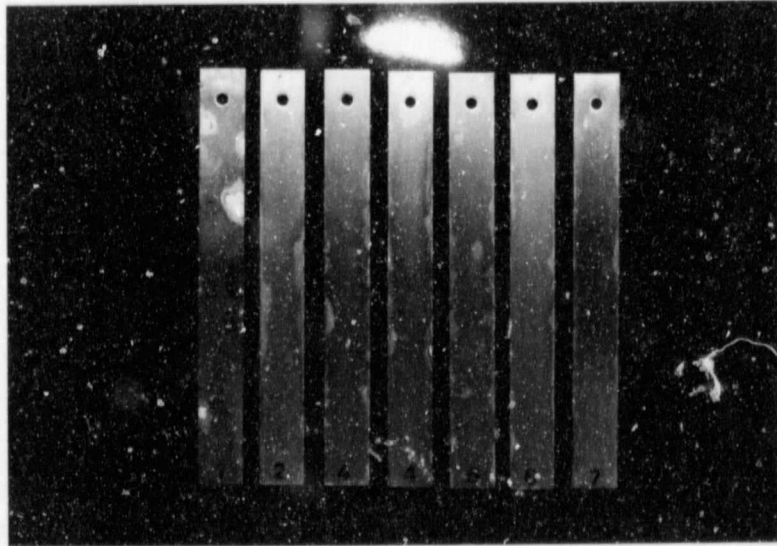


Figure 46. "Polished finish" specimens exposed in static ERPM water: 40°C, after cleaning.

There are far more pits on the "mill finish" alloys 3004 and 5251 than on their polished counterparts. However, this trend was reversed with alloy 6063TB. As noted before, there is no way that the different "mill finishes" can be vigorously compared. Differences in the processing variables may greatly effect the surface of the material. Thus the comparison between the "mill finish" and polished finish specimens is essentially an empirical one.

#### 6.1.6.1 Pit depth results

The average pit depth results are summarised in the table below.

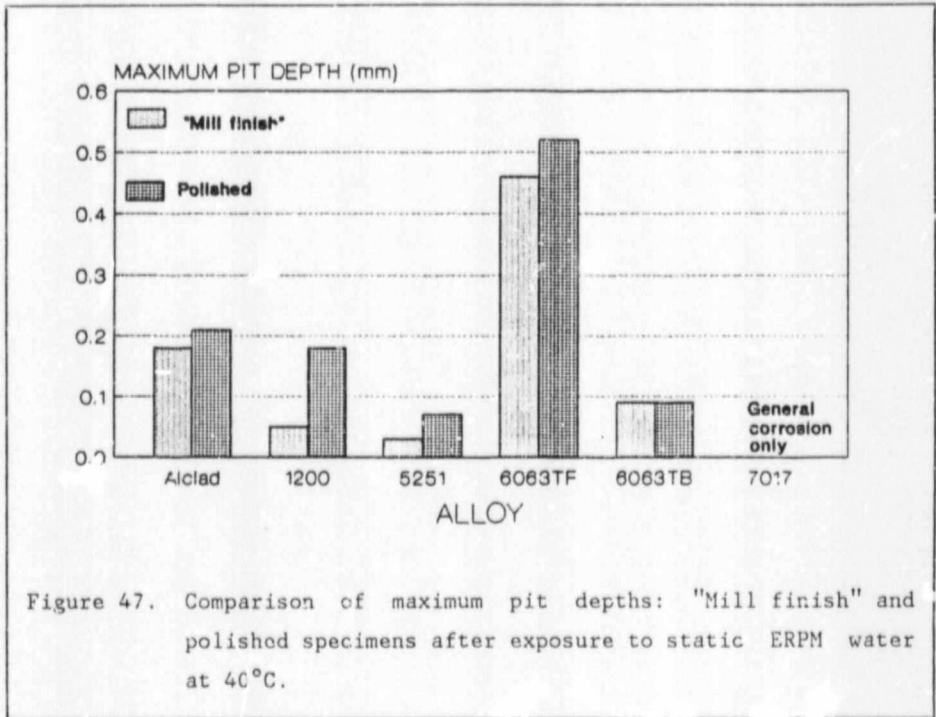
Table 6.8 Pit depths on specimens immersed in static Hercules Shaft Water at 40°C.

Alloy	Average Pit Depth (mm)	Maximum Pit Depth (mm)	Std. Deviation
<u>Mill Finish</u>			
Alclad	0,13	0,18	0,02
1200	0,02	0,05	0,01
5251	<0,01	0,03	-
6063TB	0,34	0,46	0,08
6063TF	0,06	0,09	0,03
7017	*	*	-
<u>Polished</u>			
Alclad	0,16	0,21	0,03
1200	0,08	0,18	0,04
5251	0,03	0,07	0,03
6063TB	0,30	0,52	0,51
6063TF	0,06	0,09	0,03
7017	*	*	-

The maximum pit depths are shown graphically in Figure 47 below.

---

\* - general corrosion only



It can be therefore be concluded that although generally more pits had initiated on the "mill finish" specimens, the penetration rates were lower. In other words the total corrosion current is spread out over a larger surface area i.e. the current densities were lower. The higher number of pits was expected, as there were numerous scratches on these specimens.

#### 6.1.6.2 Corrosion rate results - static conditions.

The corrosion rates calculated from the mass loss of the specimens are given below.

Table 6.9 Corrosion rates from total immersion tests in static Hercules Snart Water at 40°C.

Alloy	Corrosion Rate ( $\mu\text{m}/\text{year}$ )
<u>Mill finish*</u>	
Alclad	26,4
1200	15,4
5251	22,7
6063TB	20,4
6063TF	16,5
7017	45,8
<u>Polished**</u>	
Alclad	47,9
1200	20,9
5251	29,6
6063TB	22,9
6063TF	20,6
7017	55,1

A higher general corrosion rate for polished specimens can be expected over that for the "mill finish" specimens. Godard (7) reported lower corrosion rates for alloys where the passive film had formed in pure water before being exposed to some other medium, and the film grows faster in water than in air. The "mill finish" specimens had at least 6 months to develop the film to its maximum thickness. The levels of pollution by aggressive species such as chlorides was most likely low while the film thickened with time. The polished specimens were immersed within a few days of preparation. Hence the film may still have not reached its maximum thickness and thus on exposure to the water, the inclusion of contaminants in the passive film was likely. Thus these specimens would have had a less

---

\* - 1 set of specimens only, \*\* - average of 2 sets of specimens

Table 6.9 Corrosion rates from total immersion tests in static Hercules Shaft Water at 40°C.

Alloy	Corrosion Rate ( $\mu\text{m}/\text{year}$ )
<u>Mill finish*</u>	
Alclad	26,4
1200	15,4
5251	22,7
6063TB	20,4
6063TF	16,5
7017	45,8
<u>Polished**</u>	
Alclad	47,9
1200	20,9
5251	29,6
6063TB	22,9
6063TF	20,6
7017	55,1

A higher general corrosion rate for polished specimens can be expected over that for the "mill finish" specimens. Godard (7) reported lower corrosion rates for alloys where the passive film had formed in pure water before being exposed to some other medium, and the film grows faster in water than in air. The "mill finish" specimens had at least 6 months to develop the film to its maximum thickness. The levels of pollution by aggressive species such as chlorides was most likely low while the film thickened with time. The polished specimens were immersed within a few days of preparation. Hence the film may still have not reached its maximum thickness and thus on exposure to the water, the inclusion of contaminants in the passive film was likely. Thus these specimens would have had a less

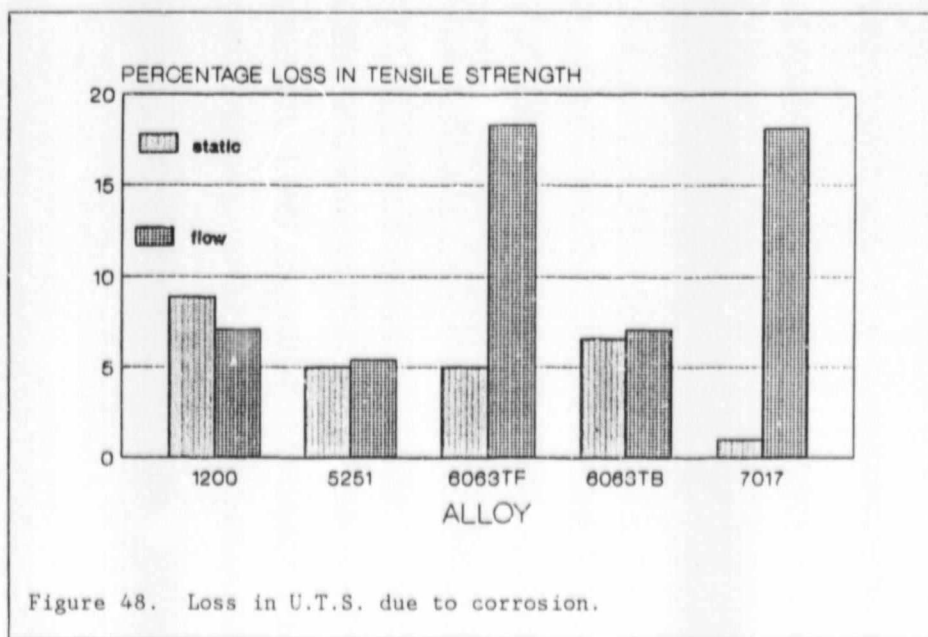
---

\* - 1 set of specimens only, \*\* - average of 2 sets of specimens

homogenous, and initially thinner passive layer, and so had lowered corrosion resistance.

### 6.1.7 TENSILE TESTS

The results from these tests are shown in Figure 48. The percentage change in the ultimate tensile strength (UTS) for Alclad is not shown as in each case there was a strength increase. This will be discussed later in section 6.2.7. The known experimental error in these tests was approximately 2,5% and to this must be added the distribution of the pits in the specimen, i.e. a pit at the edge of a specimen creates a far higher stress concentration effect than one away from the edge. However, these tests do give an idea of the degree of loss in mechanical properties that are caused by corrosion.





## 6.2 TESTS CONDUCTED IN FREDDIES NO. 5 SHAFT WATER

This mine water is typical of the Orange Free State being high in chlorides and high in sulphates. Pitting can be expected at this chloride level. The pH of the water was initially neutral at 7,2 and varied up to a maximum of 7,7 in the flow loop and down as far as a minimum of 6,85 in the static immersion tanks. This effect is related to the level of dissolved CO<sub>2</sub>. Table 6.10 gives the water analysis results.

Table 6.10 Analysis of Freddies No.5 Shaft Mine Water.

Component	Concentration*
pH	7,32
Total Hardness	1356
Ca Hardness	1118
Total Alkalinity	64
TDS	469
LSI	0,54
RSI	6,24
Chloride	1652
Calcium	448
Magnesium	58
Sodium	1050
Sulphate	2000
Nickel	2,30
Copper	0,20
Conductivity	670ms/m

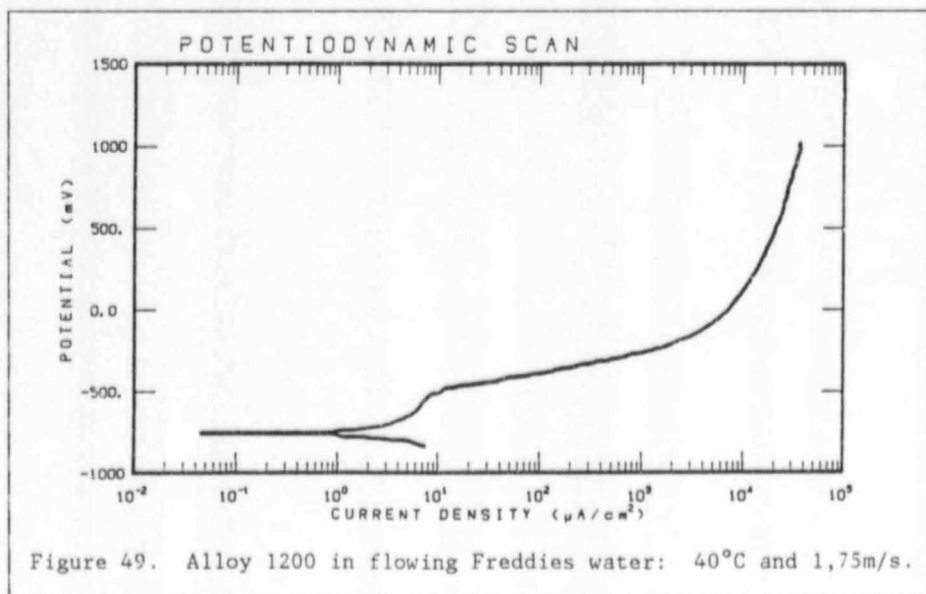
---

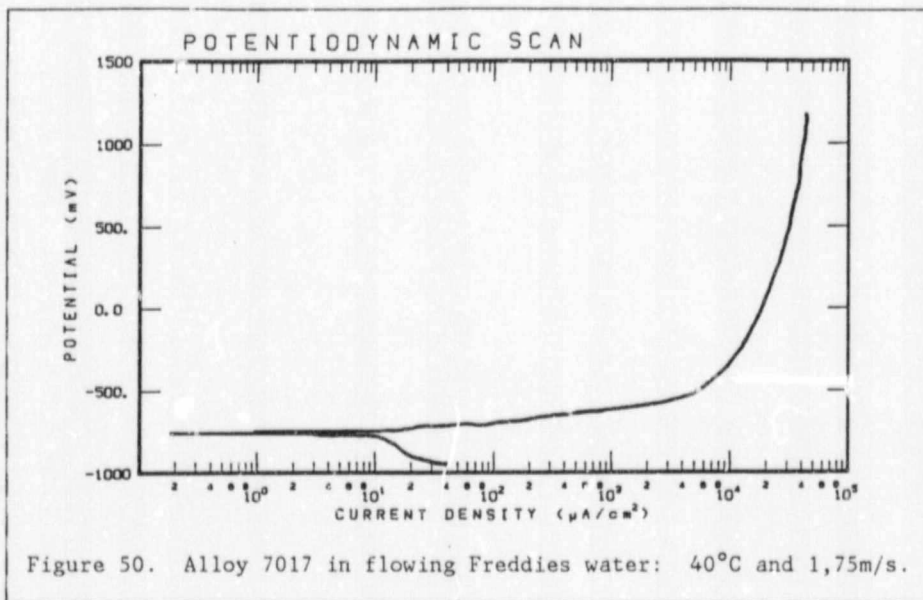
\* - in ppm where applicable

This pH is within the range (4,5 - 8,5), the levels at which the oxide layer formed on aluminium is stable, so that general corrosion is not likely to be significant.

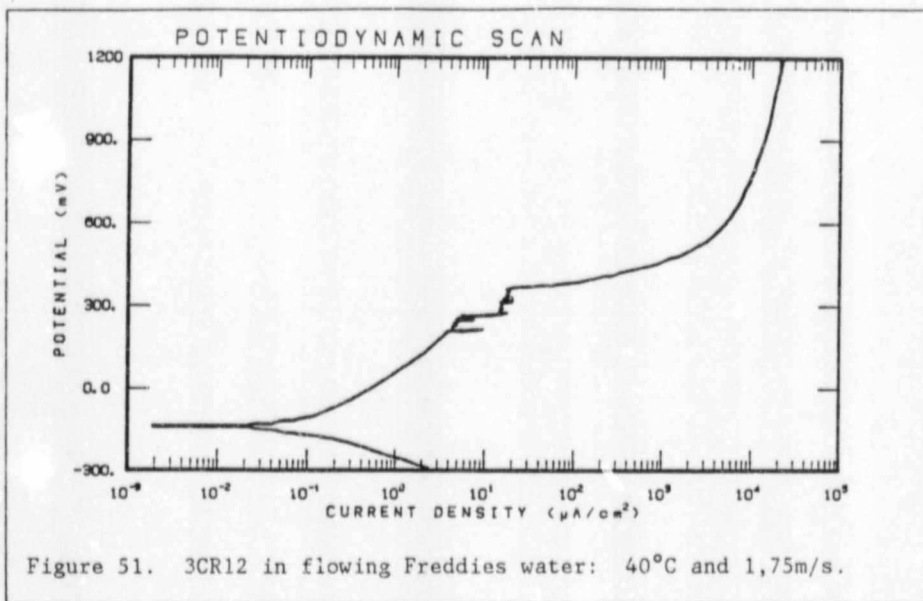
### 6.2.1 POTENTIODYNAMIC CORROSION SCANS - FLOW CONDITIONS

All of the aluminium alloys confirmed the statement above, on stable film formation, except for alloy 7017. They exhibit a region of passivity on the potentiodynamic curve, even though this region was fairly limited in most cases. Figure 49 shows this behaviour, but note that here the passive range is only of the order of 200mV, with the pitting potential  $E_{pp}$  being -540mV. Alloy 7017 showed no passivity whatsoever, as did mild steel in this water. Figure 50 shows a typical curve where no spontaneous passivation took place.

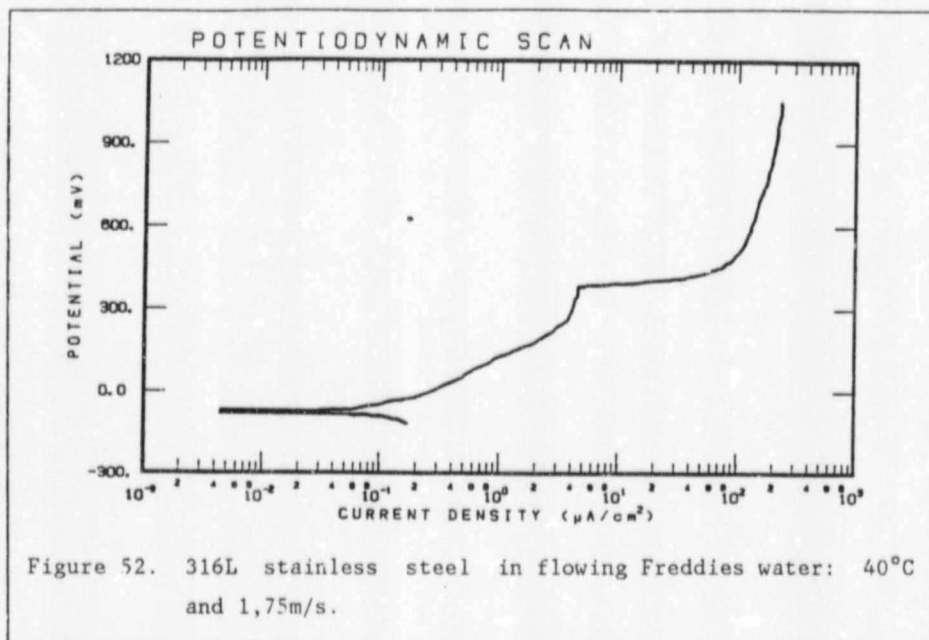




3CR12 showed a limited passive range of around 400mV with  $E_{pp} = 263\text{mV}$ . Figure 51 shows the behaviour of the alloy in this environment and it is interesting to note the "noise" on the curve around  $E_{pp}$ . This was repeatedly found with this alloy and indicates breakdown and then repair of the passive film. i.e. even before  $E_{pp}$  is reached, the film has become somewhat unstable.

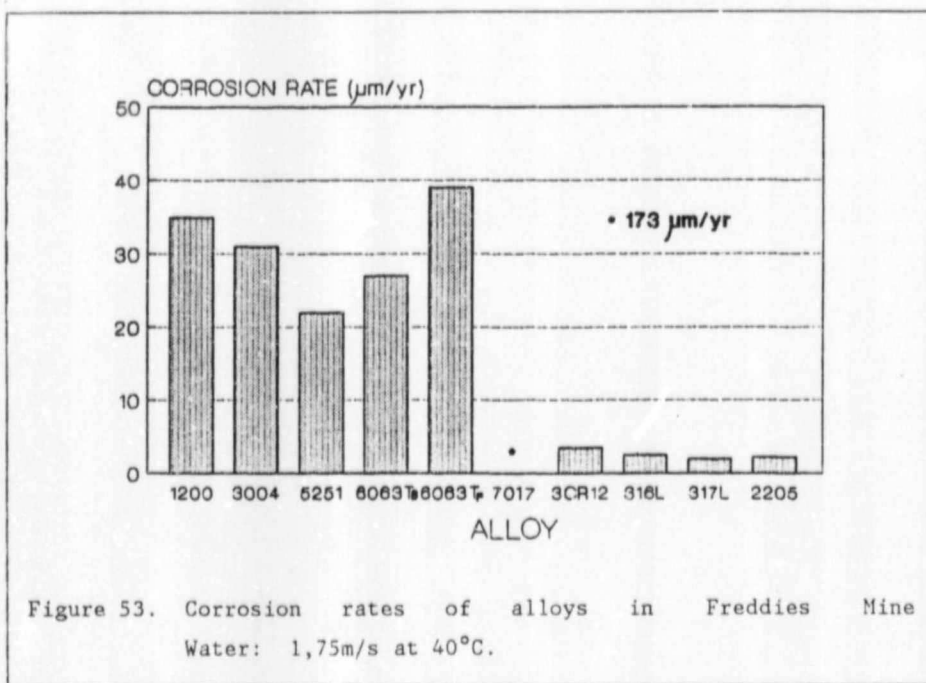


For comparison purposes limited tests were carried out on three stainless steels viz. types 316L, 317L and SAF2205. Even these alloys had fairly limited passive regions under flow conditions in this water, Figure 52 shows the potentiodynamic curve for type 316L stainless steel. It shows that spontaneous passivation took place up to 375mV ( $E_p$ ), but above this potential breakdown of the passive film would lead to pitting. Types 317 and 2205 stainless steels exhibited similarly shaped potentiodynamic curves.



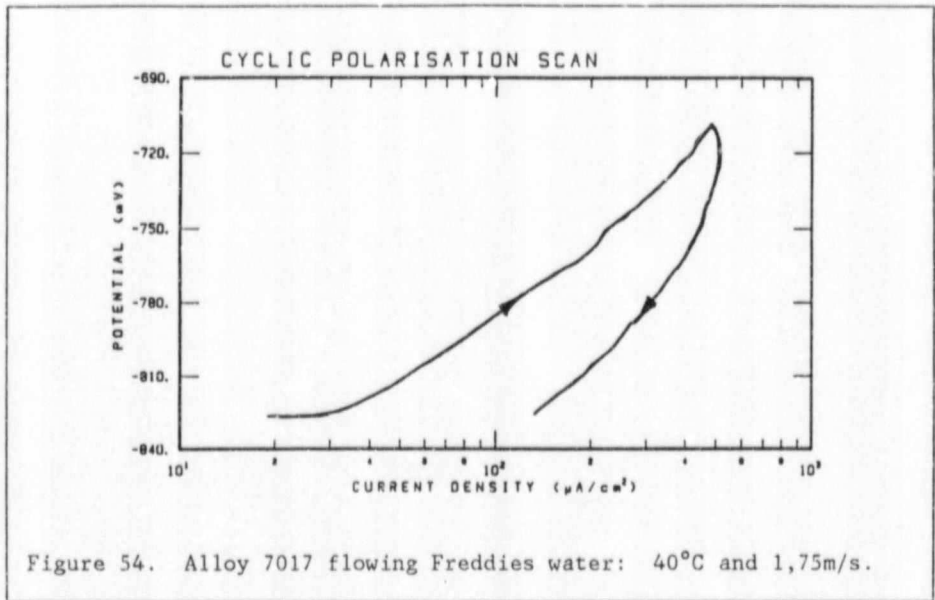
Corrosion rates for the aluminium alloys were within the range 20 to 40µm/year except for alloy 7017 which had a corrosion rate of 173µm/year. 3CR12 and the three stainless steels gave corrosion rates in the range 0,5 to 1,8µm/year - a factor of 25x lower. The **general** corrosion rates of the stainless steels are so low as to be negligible, while the aluminium alloys can be classed as "fairly resistant". Except for alloy 7017, little **general corrosion** can be expected in this type of water.

The average corrosion rates for each of the test materials except for 7017 are shown in Figure 53.

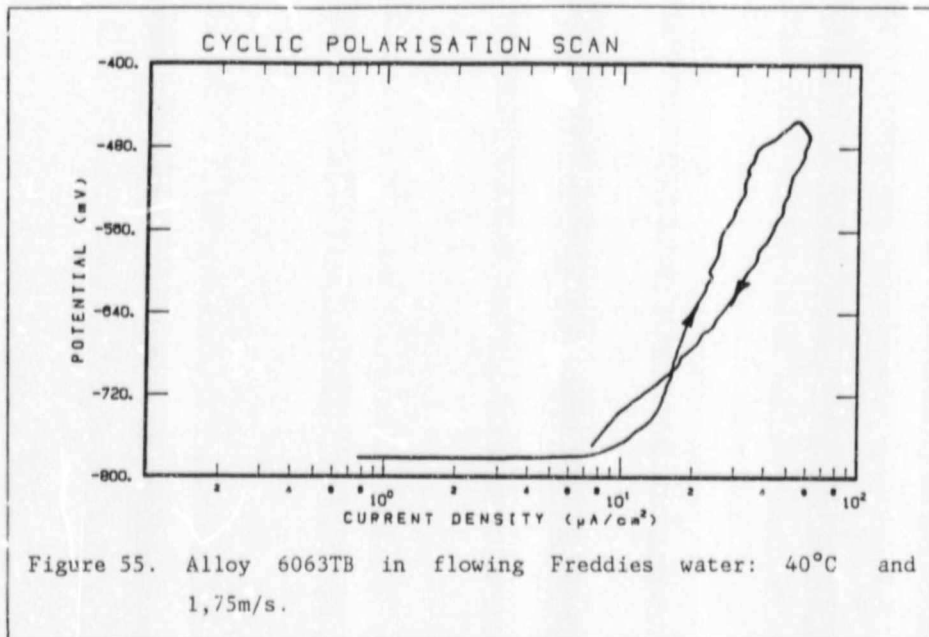


### 6.2.2 CYCLIC POLARISATION SCANS - FLOW CONDITIONS

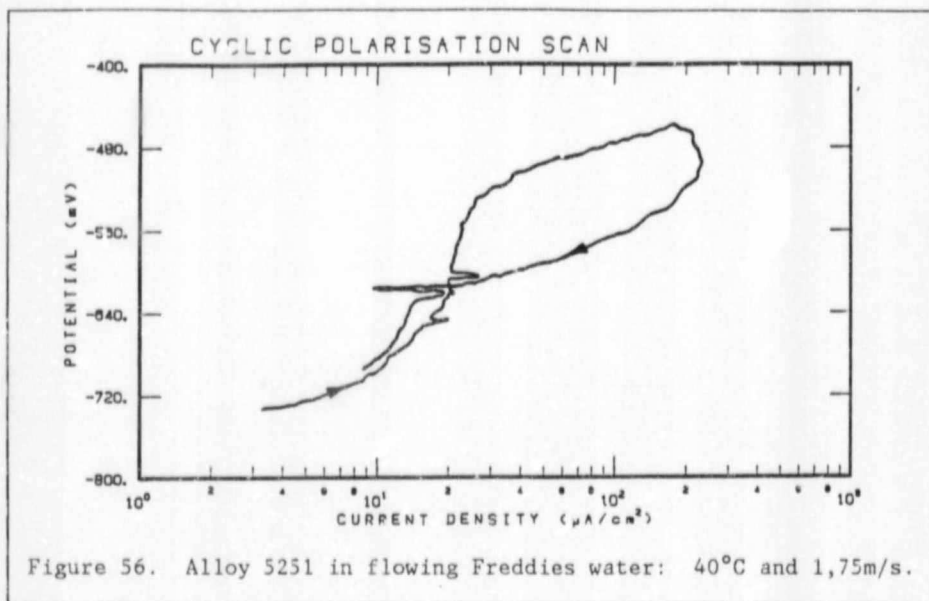
As was expected from the high concentrations of sulphate and chloride ions, pitting corrosion was the dominant mode of damage suffered by these aluminium alloys. Alloy 7017 showed no sign of passivity and the return curve of the cyclic polarisation scan remained well to the right of the forward curve. Figure 54 shows this and the large current rise with such a small potential change. Alloy 1200 does not re-passivate during the reverse scan. Alloy 6063TF shows similar behaviour.



Alloy 6063TB just re-passivates before  $E_{\text{corr}}$  is reached on the reverse scan (Figure 55). However this gives a perfectly passive region of only 83mV out of a passive range of 313mV. It is also very important to note that the whole curve is at highly anodic potentials.



The reverse curve intersects the forward curve on the pitting scans for both 3004 and 5251. Alloy 3004 has a passive range of 160mV and a perfectly passive range of 70mV; too limited for use in this environment. Alloy 5251 is slightly better with passive and perfectly passive ranges of 200mV and 116mV respectively - still extremely limited. Figure 56 shows the pitting curve for alloy 5251. Both these alloys exhibit a large hysteresis loop in the pitting curve and hence they have low resistance to crevice corrosion.



3CR12 managed to re-passivate in some tests but in others it did not. This indicates that it is a "borderline" situation for this alloy and very small changes in the test environment/procedure can make a big difference in the result. The stainless alloys all managed to re-passivate once pitting had initiated. Figure 57 shows a pitting curve for type 316L stainless steel. The reverse scan intersected the forward curve at 262mV and so the regions of passivation and perfect passivation are 488mV and 318mV respectively. The hysteresis loop indicates poor crevice corrosion resistance even, for these highly alloyed materials.

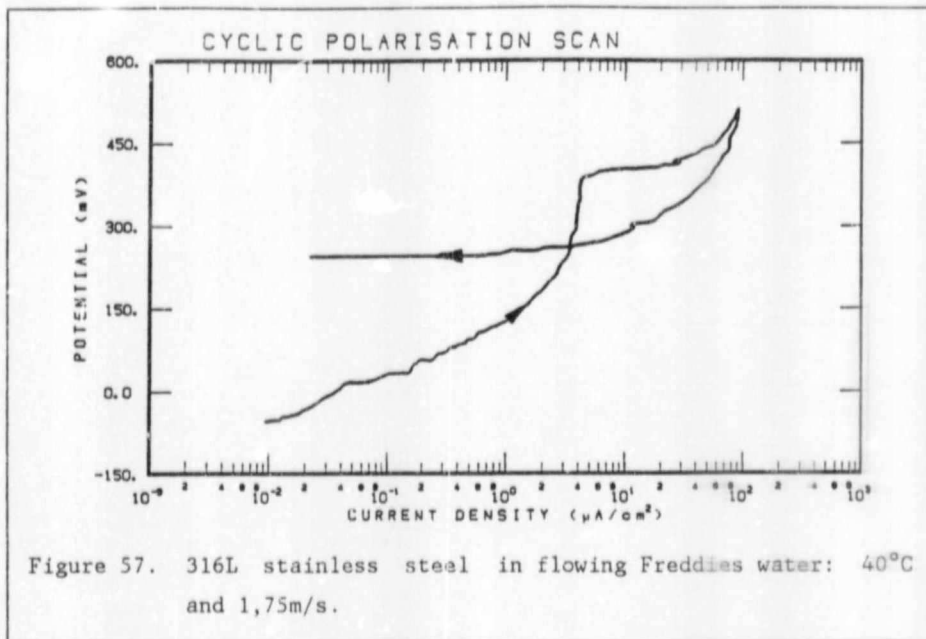
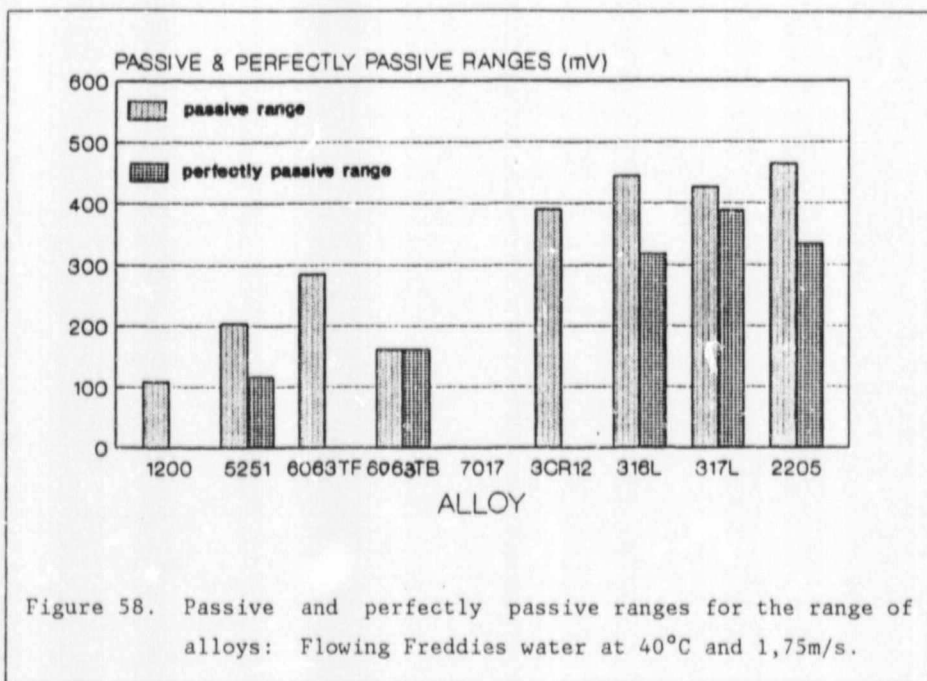


Table 6.11 summarises the data gained from the pitting scans, whilst the passive and perfectly passive ranges are shown graphically in Figure 58.



**Author** Buchan Andrew John

**Name of thesis** Corrosion Of Aluminium Alloys In Static And Recirculating Mine Waters. 1988

***PUBLISHER:***

University of the Witwatersrand, Johannesburg

©2013

***LEGAL NOTICES:***

**Copyright Notice:** All materials on the University of the Witwatersrand, Johannesburg Library website are protected by South African copyright law and may not be distributed, transmitted, displayed, or otherwise published in any format, without the prior written permission of the copyright owner.

**Disclaimer and Terms of Use:** Provided that you maintain all copyright and other notices contained therein, you may download material (one machine readable copy and one print copy per page) for your personal and/or educational non-commercial use only.

The University of the Witwatersrand, Johannesburg, is not responsible for any errors or omissions and excludes any and all liability for any errors in or omissions from the information on the Library website.